Cavity magnonics with domain walls in insulating ferromagnetic wires

Mircea Trif[1,*] and Yaroslav Tserkovnyak[2]

[1]*International Research Centre MagTop, Institute of Physics, Polish Academy of Sciences, Aleja Lotnikow 32/46, PL-02668 Warsaw, Poland*

[2]*Department of Physics and Astronomy and Bhaumik Institute for Theoretical Physics, University of California, Los Angeles, California 90095, USA*

(Received 6 March 2024; revised 19 September 2025; accepted 30 January 2026; published 5 March 2026)

Magnetic domain walls (DWs) are topological defects that host robust low-energy modes, which can be harnessed for classical and neuromorphic computing. However, accessing their quantum dynamics has remained an outstanding challenge. Using concepts from cavity optomechanics, we show that a geometric, Coriolis-type interaction between localized DWs and extended magnon modes in short insulating ferromagnetic wires enables efficient cooling of DWs to their quantum ground state and the preparation of nonclassical states with negative Wigner functions, detectable in the power spectrum of emitted magnons. We further demonstrate that magnons can mediate long-range entangling interactions between qubits encoded in spatially separated DWs, providing a route toward universal quantum gate operations. Our proposal relies solely on intrinsic degrees of freedom of the ferromagnet and naturally extends to ferrimagnets and antiferromagnets, as well as to other confined magnetic textures such as vortices and skyrmions in insulating nanostructures.

DOI: 10.1103/h876-wl85

I. INTRODUCTION

Magnetic domain walls (DWs) are stable topological magnetic configurations that are robust against local deformations [1]. Because of their topological stability, capacity for high-density packing, and flexible design, magnetic DWs in ferromagnetic nanowires have emerged as a promising avenue for data storage and information processing in spintronic devices [2–6]. Understanding their dynamics and motion is crucial for achieving high-speed operation and the efficient manipulation of spintronic devices.

Miniaturization naturally raises the question of the importance of quantum effects in future DW-based devices. Indeed, several works have recently proposed harnessing their quantum properties in order to encode and process quantum information at the nanoscale [7–12]. However, such endeavors require the DW to be in the ground state, or at least near its ground state. Until now, no such achievement has been demonstrated experimentally, largely because the required operating temperatures are too low (∼mK). This raises the question of whether the quantum regime can be reached in practice and, if so, under what conditions? In this work, we answer these questions affirmatively by proposing a ground-state cooling method that exploits the intrinsic magnons (or spin waves) in insulating ferromagnetic devices hosting DWs. We focus on a finite ferromagnetic insulating wire of length $2L$ and easy-axis anisotropy K_e that harbors one (or several) DW(s) of size $\lambda \ll L$ along its length, as depicted in Fig. 1. When the DW is pinned in the z direction, the low-energy spectrum is determined by the dynamics of the collective coordinate Φ, which parametrizes the angle of the spin texture of the DW [13]. The resulting (quantum) level structure can be manipulated by an external magnetic field $\boldsymbol{B}$ that modifies the confining potential $U(\Phi)$ (see Fig. 1), rendering it highly anharmonic. Therefore, the two lowest energy levels localized at the DW, $\{|1\rangle, |2\rangle\}$, can be used to encode a qubit below the

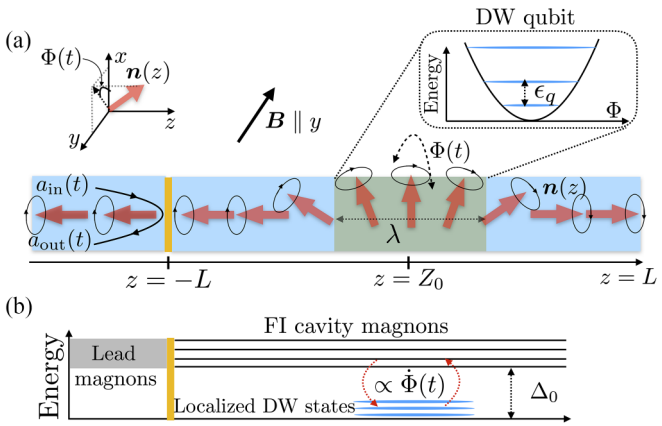


FIG. 1. Magnonic cavity with a DW. (a) A ferromagnetic insulator (FI) wire of length $2L$ and magnetization profile $\boldsymbol{n}(z)$ harbors a DW of size $\lambda \ll L$ pinned at position Z_0 in the wire. An external magnetic field $\boldsymbol{B} \parallel y$ controls the DW spectrum, permitting the encoding of a qubit with energy ϵ_q in the two lowest levels. (b) The magnons have a gap Δ_0 from the easy-axis z anisotropy and couple to the DW with strength $\propto \dot{\Phi}(t)$. Driving the FI cavity magnons externally, e.g., by coupling them to a precessing magnonic lead, facilitates the manipulation [by the input magnons $a_{\rm in}(t)$] and the detection [from the power spectrum of the output magnons $a_{\rm out}(t)$] of the DW levels.

*Contact author: mtrif@magtop.ifpan.edu.pl

Published by the American Physical Society under the terms of the Creative Commons Attribution 4.0 International license. Further distribution of this work must maintain attribution to the author(s) and the published article's title, journal citation, and DOI.

gapped magnonic levels [8,12]. However, the external magnetic field, in-plane anisotropies, and—most importantly—the DW rotational motion induce interactions between the localized DW states and the gapped, extended magnons, which in turn alter their collective dynamics. Instead of viewing this as a nuisance, here we harness such interactions to control the DW dynamics. Using the theoretical framework of cavity optomechanics [9,14–19], we find that the large anharmonicity of the DW (supplemented by dissipation) in the presence of coherently driven magnons enables means of controlling the motion of the DW at the quantum level. Specifically, we advance the conditions for efficient cooling to the ground state as well as prepare stationary DW states that exhibit a negative Wigner function—a hallmark of a pure quantum regime. Experimentally, such features can be extracted from the power spectrum of the emitted magnons.

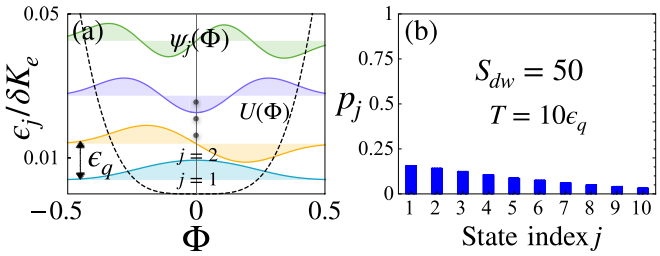


FIG. 2. (a) The DW energy levels ϵ_j and wave functions $\psi_j(\Phi)$, with $j = 1, 2, \ldots$, for a reduced magnetic field $\tilde{b} = \pi b/2K_h = 1$ leading to a quartic effective potential $U(\Phi)$ (dashed line). (b) Occupation of DW levels for $T = 10\epsilon_q$, indicating a highly thermal (or classical) state. The other parameters are $\widetilde{K}_h = 5\delta K_e$ and $S_{\rm dw} = 50$, while all energies are expressed in terms of δK_e.

II. PHENOMENOLOGY OF DW-MAGNON DYNAMICS

To grasp the essentials of our proposal, we start with a heuristic discussion of our main findings, relegating the technical details to later sections and the Supplemental Material [20]. A DW is described by the collective (and canonically conjugate) coordinates Z and Φ [13], denoting its position (scaled by λ) and the rotation angle in the wire, respectively. In the presence of a strong pinning potential $V_{\rm pin}(Z) = \delta K_e(Z - Z_0)^2/2$, with δK_e being its strength, the motion along z is quenched, and the low-energy dynamics of a DW with spin $S_{\rm dw}$ (per unit length λ) are described by the following rotational Hamiltonian ($\hbar = 1$):

$$H_\Phi = \frac{1}{2M_\Phi}P_\Phi^2 + U(\Phi). \tag{1}$$

Here, $M_\Phi = (2S_{\rm dw})^2/\delta K_e$ and P_Φ are the mass of the DW and the canonical momentum associated with rigid rotations of the DW, respectively, while $U(\Phi)$ describes the potential that depends on the magnetic anisotropies and the external magnetic field. The latter can adjust $U(\Phi)$ from a double-well potential to a single-well potential that is harmonic in nature [12]. Promoting the momentum to a quantum variable, i.e., $P_\Phi \to -i\partial_\Phi$, allows us to solve the Schrödinger equation $H_\Phi\psi_j(\Phi) = \epsilon_j\psi_j(\Phi)$, with $\psi_j(\Phi)$ and ϵ_j being, respectively, the eigenstate and energy of mode $j = 1, 2, \ldots$ of the DW. Importantly, the anharmonicities facilitate the implementation of a qubit in the subspace spanned by the two lowest energy levels with splitting $\epsilon_q \equiv \epsilon_2 - \epsilon_1$ [8,12].

When the external magnetic field is adjusted to make the potential quartic, $U(\Phi) \approx \widetilde{K}_h\Phi^4/4$, both the qubit splitting and the anharmonicity are governed by $\widetilde{K}_h$, which denotes the effective hard-axis anisotropy of the domain wall along the y direction [20]. The resultant spectrum and wave functions are shown in Fig. 2 (a). We can gain further insight into the anharmonicity in this limit by using the quasiclassical Bohr-Sommerfeld quantization condition [20] to find $\epsilon_j \approx \epsilon_1(j - 1/2)^{4/3}$, with $j = 1, 2, \ldots$ and

$$\epsilon_1 \approx \frac{0.86}{S_{\rm dw}^{4/3}}\left(\widetilde{K}_h\delta K_e^2\right)^{1/3}. \tag{2}$$

To provide some estimates, for a DW with $S_{\rm dw} \approx 50$, $\widetilde{K}_h = 5\delta K_e$, and $\delta K_e \approx 10\,$GHz, we find a qubit splitting of $\epsilon_q \approx 10^{-2}\delta K_e \approx 100\,$MHz. We stress that it is possible to achieve larger qubit splittings by selecting ferrimagnetic wires that are close to the compensation point, $S_{\rm dw} \approx 0$ [12].

The decoherence of the DW quantum levels can be accounted for by substituting $H_\Phi \to H_\Phi - \Phi\xi(t)$, where $\xi(t)$ is the Langevin force obeying the fluctuation-dissipation condition $\langle\xi(t)\xi(0)\rangle = \alpha S_{\rm dw}\int(d\omega/2\pi)e^{-i\omega t}\omega\coth(\omega/2k_BT)$ at a temperature T, with k_B as the Boltzmann constant and α the Gilbert damping [7]. In a quantum description, it corresponds to a bosonic bath that discriminates between the emission and absorption processes. The transition rate $\gamma_{\rm jk}$ from state j to state k can be evaluated using Fermi's golden rule [21], giving $\gamma_{\rm jk} = \alpha S_{\rm dw}|\langle j|\Phi|k\rangle|^2\epsilon_{\rm jk}[1 + \coth(\epsilon_{\rm jk}/2k_BT)]$, with $\epsilon_{\rm jk} = \epsilon_j - \epsilon_k$, while $\gamma_{\rm kj} = \gamma_{\rm jk}\exp(-\epsilon_{\rm jk}/k_BT)$, in thermal equilibrium. Using the same qubit parameters, and $\alpha = 10^{-5}$ [7], we find $\gamma_{12} \sim \gamma_{21} \approx 10^{-3}\epsilon_q$ for $T = 0.05\,$K ($\approx 10\epsilon_q$). Although the qubit exhibits low relaxation rates, the occupation of the DW levels at $T = 0.05\,$K is highly thermal, as shown in Fig. 2(b), thus far from its ground state, as desired for qubit initialization.

Next, we qualitatively discuss the interaction with the magnons, fluctuations around the localized DW that extend throughout the wire [22], which can be used to cool the DW toward its ground state. In a frame rotating with the DW, the magnons are subject to a fictitious magnetic field pointing along the wire axis $B_{\rm m}(Z_0) \propto \dot{\Phi}\, m_{\rm dw}$, with $m_{\rm dw} = (N_{\leftarrow} - N_{\rightarrow})/N_{\rm tot} \equiv Z_0/L$ being the spin-up/spin-down fraction of the magnon (which moves ballistically across the DW), $N_{\leftarrow(\rightarrow)}$ the number of spins pointing in the left (right) direction, while $N_{\rm tot} = N_{\leftarrow} + N_{\rightarrow}$ [23]. Physically, the DW rotation defines a non-inertial frame for the spin fluctuations, giving rise to a velocity-dependent, Coriolis-type force acting on the magnons. Its physical manifestations are revealed when driving the magnons externally close to their respective ferromagnetic resonance (which can be achieved, for example, by driving the magnons directly with microwaves or by coupling them to a precessing ferromagnetic lead, as shown in Fig. 1). In the rotating frame, the driving Hamiltonian acquires a phase $\exp(i\Phi)$, which can be eliminated via a gauge transformation, leading to an effective magnetic field $B_{\rm m} \to B'_{\rm m} \propto \dot{\Phi}(1 - m_{\rm dw})$ acting on the cavity magnons. In a Hamiltonian description, this velocity-dependent coupling corresponds to a vector potential that acts on the magnons [20], with a

maximum (minimum) strength at $Z_0 = -L$ ($Z_0 = L$). If a specific magnonic mode of energy ω_n is triggered by an external drive of frequency Ω_n and strength h_n at the left end, only this mode effectively participates in the dynamics. Then, we arrive at the following DW-magnon coupling Hamiltonian:

$$H_{\rm tot} \approx \frac{(P_\Phi - P_n a_n^\dagger a_n)^2}{2M_\Phi} + \Delta_n a_n^\dagger a_n + h_n(a_n^\dagger + a_n), \qquad (3)$$

where a_n ($a_n^\dagger$) are the annihilation (creation) operators for the magnon mode with energy $\Delta_n \equiv \omega_n - \Omega_n$, while $P_n \equiv P_n(Z_0) \approx 1 - m_{\rm dw}$ [24]. Equation (3) is formally analogous to an optomechanical system, with the DW angle and the magnons replacing the mechanical position and the cavity photons, respectively [14]. Note that in the absence of the drive ($h_n = 0$), the coupling is a pure gauge shift and is, therefore, inconsequential. Equation (3) is one of our central results and serves as the starting point for analyzing the quantum dynamics of macroscopic domain-wall degrees of freedom. We also emphasize that the short-wavelength adiabatic transport regime commonly discussed in the literature [25–27] is distinct from the long-wavelength, confined quantum regime considered here. Next, we provide a microscopic derivation linking the Coriolis-type interaction to the geometric Wess-Zumino (WZ) term of the spin Lagrangian.

III. MICROSCOPIC MODEL

We assume that the ferromagnetic wire is well below the Curie temperature T_c, such that the long-wavelength dynamics can be described in terms of coarse-grained continuous fields $\boldsymbol{n}(z) = \{\sin\theta\cos\phi, \sin\theta\sin\phi, \cos\theta\}$. The Lagrangian for the magnetic wire reads [13]

$$\mathcal{L}[\boldsymbol{n}, \dot{\boldsymbol{n}}] = -\int_{-L}^{L} dz \left(s \frac{\boldsymbol{d}\times\boldsymbol{n}}{1+\boldsymbol{n}\cdot\boldsymbol{d}} \dot{\boldsymbol{n}} + \mathcal{H}_F[\boldsymbol{n}] \right),$$
$$\mathcal{H}_F[\boldsymbol{n}] = \frac{1}{2}\left[A(\partial_z \boldsymbol{n})^2 - K_e n_z^2 + K_h n_y^2 + b n_y \right], \qquad (4)$$

where $\boldsymbol{d}$ is the (arbitrary) direction of the Dirac string, while s, A, K_e, K_h, and b represent the spin density, exchange (stiffness), easy-axis anisotropy, hard-axis anisotropy, and magnetic field, respectively. To account for dissipation consistent with the Landau-Lifshitz-Gilbert (LLG) equation governing the magnetization dynamics, the above Lagrangian can be supplemented with the Rayleigh function $\mathcal{R}[\dot{\boldsymbol{n}}] = \alpha s \int dz \dot{\boldsymbol{n}}^2(z)/2$.

In the absence of an external magnetic field, the ferromagnet has two classical ground states, $\boldsymbol{n}(z) = \pm\boldsymbol{e}_z$, which are uniformly polarized along the easy axis. Additionally, in the limit $L \to \infty$, the model above admits a DW solution $\boldsymbol{n}_0$ that minimizes the Hamiltonian part [second term in Eq. (4)] for boundary conditions $\boldsymbol{n}_0(z = \pm\infty) = \pm\boldsymbol{e}_z$:

$$\cos\theta_0(z) = \tanh[Q(z - Z)], \quad \phi(z) \equiv \Phi, \qquad (5)$$

where $Q = \int_{-\infty}^{\infty} dz \partial_z\theta/\pi = \pm 1$ is the topological charge determined by the boundary conditions (at the edges of a long wire), while Z and Φ are the unconstrained position and angle of the domain wall, with all lengths expressed in terms of $\lambda \equiv \sqrt{A/K_e}$. The low-energy dynamics of the DW for b, $K_h \neq 0$ is described by the Lagrangian [13]

$$\mathcal{L}_{\rm dw} = -2S_{\rm dw} Z\dot{\Phi} + U(\Phi) - V_{\rm pin}(Z),$$
$$U(\Phi) = \widetilde{K}_h(\sin^2\Phi + \tilde{b}\sin\Phi), \qquad (6)$$

where $S_{\rm dw} = s\lambda$, $\widetilde{K}_h = K_h\lambda$, $\tilde{b} = \pi b/2K_h$, we also introduced a pinning potential $V_{\rm pin}(Z) = -(\delta K_e/2)\cosh^{-2}(Z - Z_0)$, stemming from a pointlike defect at position Z_0 that causes a local reduction of the easy-axis anisotropy by $\delta K_e (> 0)$ [13]. Using $P_\Phi = \partial_{\dot\Phi}\mathcal{L}_{\rm dw} = -2S_{\rm dw}Z$ and $P_Z = \partial_{\dot Z}\mathcal{L}_{\rm dw} = 0$, we can identify that $\{Z, \Phi\}$ are canonically conjugate variables. In the limit of strong pinning $\delta K_e \gg \widetilde{K}_h \max(1, \tilde{b})/S_{\rm dw}^2$ (but $\delta K_e \ll \widetilde{K}_e \equiv K_e\lambda$), Z becomes a purely harmonic variable defining the inertia of generally nonlinear dynamics of Φ, which is governed by Eq. (1). We note that we performed micromagnetic simulations with comsol (LLG dynamics) to confirm that the DW is only weakly distorted by the external magnetic field and to validate the effective DW Hamiltonian [20].

In the presence of high-frequency fluctuations, the magnetization profile can be written as $\boldsymbol{n}(z,t) = \boldsymbol{n}_0(z - Z) + \delta\boldsymbol{n}(z,t)$, where $\boldsymbol{n}_0$ is the static DW solution and $\delta\boldsymbol{n} \perp \boldsymbol{n}_0$ represents magnon modes. Expanding the fluctuations in the local orthogonal basis $\boldsymbol{e}_1 = \partial_{\theta_0}\boldsymbol{n}_0$, $\boldsymbol{e}_2 = \sin^{-1}\theta_0\,\partial_\Phi\boldsymbol{n}_0$, we obtain $\delta\boldsymbol{n} = \boldsymbol{e}_1\,\delta n_1 + \boldsymbol{e}_2\,\delta n_2$ with small amplitudes $\delta n_{1,2} \ll 1$. Substituting into the Lagrangian yields three contributions, $\mathcal{L} = \mathcal{L}_{\rm dw} + \mathcal{L}_{\rm m} + \mathcal{L}_{\rm int}$, where $\mathcal{L}_{\rm dw}$ accounts for the collective DW coordinates, $\mathcal{L}_{\rm m}$ describes free magnons, and $\mathcal{L}_{\rm int}$ represents their coupling. For a fixed DW position and angle, the magnon part reduces to

$$\mathcal{L}_{\rm m} = -\frac{1}{2}\int_{-L}^{L} dz[2s\delta n_1\partial_t\delta n_2 + \delta n_1\mathcal{H}_0\delta n_1 + \delta n_2\mathcal{H}_0\delta n_2],$$
$$\mathcal{H}_0 = \widetilde{K}_e\left(-\frac{\partial^2}{\partial z^2} + 1 - 2\,\mathrm{sech}^2(z - Z)\right), \qquad (7)$$

where $\mathcal{H}_0$ is an effective Hamiltonian describing the magnons in a potential landscape $U(z) = 2\,\mathrm{sech}^2(z - Z)$. We can parametrize the magnonic field as $\delta n(z,t) \equiv \delta n_1(z,t) + i\delta n_2(z,t) = \sum_n \Psi_n(z, Z)a_n(t)$, where $\Psi_n(z, Z)$ with $n = 0, 1, \ldots$ are the standing wave solutions pertaining to a magnetic wire of length $2L$ described by $\mathcal{H}_0$, subject to the vanishing spin current at the boundaries $J_s^z \equiv \partial_z\Psi_n(\pm L, Z) = 0$, while $a_n(t)$ are the complex-valued amplitudes of the magnon in the state with energy ω_n. In a quantum description, $a_n(t)$ [$a_n^*(t)$] becomes the magnon annihilation (creation) operator that satisfies $[a_n, a_m^\dagger] = \delta_{nm}$ [20]. The corresponding standing waves of energy $\omega_n = K_e(1 + k_n^2)/s$, with the set of allowed magnonic momenta k_n, can be written as $\Psi_n(z, Z) = p_n\psi_{k_n}(z, Z) + q_n\psi_{-k_n}(z, Z)$, while $\psi_k(z, Z)$ are normalized magnon solutions in an infinite system that can be found explicitly by exploiting the property that they scatter over the potential $U(z)$ without any reflection [20,22]. When $L \gg 1$ and the DW location is far from the edges, that is, $L - |Z| \gg 1$, the boundary conditions result in the transcendental equation $\tan(2k_nL) = 2k_n/(1 - k_n^2)$, while normalization of the wave function gives $q_n = \pm p_n = 1/\sqrt{2L}$ [20]. Here, the sign + (−) corresponds to the set of solutions that satisfy $\tan(k_nL) = k_n$ [$\tan(k_nL) = -1/k_n$]. The energy separation between neighboring levels is $\Delta\omega_n \equiv \omega_{n+1} - \omega_n \approx \omega_0\pi^2(2n + 1)/L^2$. Promoting Φ to a dynamical variable results in the

following magnon-DW interaction in a frame rotating with the DW:

$$\mathcal{L}_{\rm int}(Z) = \frac{s\dot{\Phi}}{2}\int_{-L}^{L} dz\big(\delta n_1^2 + \delta n_2^2\big)\cos\theta_0, \tag{8}$$

which pertains to a fictitious magnetic field acting on the excited magnons. Neglecting intermode magnon coupling (as the corresponding terms are off-resonant), the expression reduces to the same Coriolis-type interaction between the domain wall and the excited magnons, in agreement with the phenomenological derivation presented in the previous section [28] (see also [20]).

IV. QUANTUM DYNAMICS, COOLING, AND EXCITATION OF DOMAIN WALLS

The dynamics of the wire induced by the Hamiltonian in Eq. (3), which describes the magnonic cavity in the presence of external influences (e.g., directly with microwaves or through a precessing ferromagnetic lead coupled to the wire), are captured by a Lindblad evolution of the density matrix ρ_S [29]

$$\dot{\rho}_S = i[\rho_S, H_{\rm tot}] + \kappa_n \mathcal{D}(a_n)\rho_S + \sum_{j,k}\gamma_{\rm jk}\mathcal{D}(A_{\rm jk})\rho_S, \tag{9}$$

where $\mathcal{D}(\mathcal{O})\rho_S = \mathcal{O}\rho_S\mathcal{O}^\dagger - \{\mathcal{O}^\dagger\mathcal{O}, \rho_S\}/2$ represents the dissipator associated with the jump operator $\mathcal{O}$, κ_n is the total decay rate of the magnonic mode n (including the intrinsic Gilbert damping), and $A_{\rm jk} = |k\rangle\langle j|$. Above, we retained only the emission processes in the magnonic dissipator, which is justified in the limit $\omega_0 \gg k_B T$ considered here. We can further expand the magnonic operators around their steady-state values, $a_n \to \alpha_n + a_n$, with $\alpha_n \approx -h_n/(\Delta_n - i\kappa_n/2)$, such that the resulting master equation is the same as above, but with the Hamiltonian:

$$H'_{\rm tot} \approx H_\Phi + g_n P_\Phi(a_n^\dagger + a_n) + \Delta_n a_n^\dagger a_n, \tag{10}$$

where $g_n = P_n(Z_0)|\alpha_n|/M_\Phi$ and the detunings Δ_n are slightly shifted by the DW-induced Lamb shifts of the magnons [29]. This Hamiltonian is identical to that describing (nonlinear) optomechanical setups [14] and can therefore be used to manipulate the DW states.

A first application concerns the sideband cooling of the DW levels via frequency up-conversion of the magnons, which could enable efficient initialization of the DW qubit. For efficient cooling, the following conditions must be met [14]:

$$(1)\ g_n|\langle 1|P_\Phi|2\rangle| \ll \kappa_n \ll \epsilon_q$$

$$(2)\ \gamma_{12} \ll \frac{g_n^2|\langle 1|P_\Phi|2\rangle|^2}{\kappa_n},$$

allowing us to eliminate adiabatically the magnons and ensuring that the cooling overcomes the environmental heating of the DW via the Gilbert damping, respectively. The reduced density matrix that describes the dynamics of the DW, $\rho_\Phi = {\rm Tr}_{\rm m}[\rho_S]$, acquires the same form as in Eq. (9), dictated instead by H_Φ, and the total transition rate from state j to state k becomes $\Gamma_{\rm jk}^{\rm tot} = \gamma_{\rm jk} + \Gamma_{\rm jk}^n$, where

$$\Gamma_{\rm jk}^n = \frac{1}{2}\frac{g_n^2|\langle j|P_\Phi|k\rangle|^2\kappa_n}{(\Delta_n + \epsilon_{\rm jk})^2 + (\kappa_n/2)^2}. \tag{11}$$

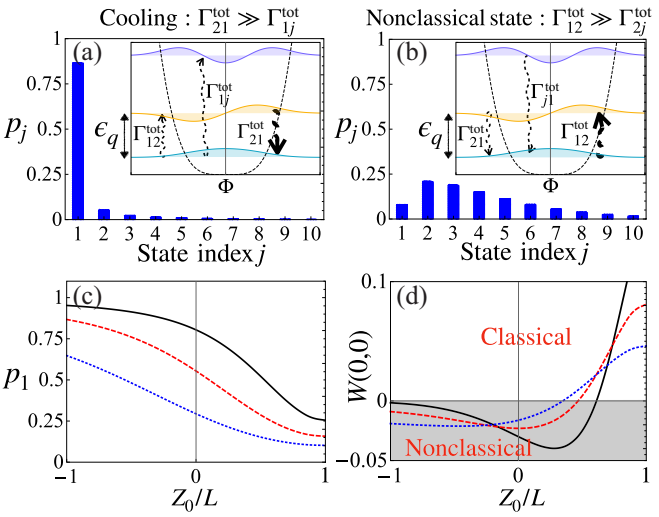


FIG. 3. (a) Occupation of the first ten DW levels when the lowest magnon ($n = 0$) is driven such that $\Delta_0 = -\epsilon_q$ and $Z_0 = -L$. (b) Same for $\Delta_0 = \epsilon_q$ and $Z_0 = 0$, resulting in a nonclassical state with negative Wigner function, $W(0,0) = -0.02$. (c) The ground-state population p_1 as a function of the position of the DW, Z_0/L, for $\Delta_0 = -\epsilon_q$ (cooling). The black, dashed red, and dotted blue curves correspond to $T = 5\epsilon_q$, $T = 10\epsilon_q$, and $T = 20\epsilon_q$, respectively. (d) The Wigner function $W(0,0)$ as a function of Z_0/L for $\Delta_0 = \epsilon_q$ (heating), with the same parameters as in panel (c); $W(0,0) < 0$ (shaded area) describes nonclassical states. Note that $Z_0 = 1$ refers to a thermal distribution because the DW-magnon interaction vanishes. Also, $|\alpha_0| = 0.1$ and $\kappa_0 = 0.1\epsilon_q$, while all other parameters are the same as in Fig. 2.

In the stationary limit, the DW density matrix becomes $\rho_\Phi = \sum_j p_j|j\rangle\langle j|$, where p_j is the occupation of the level $j = 1, 2, \ldots$. When $\Delta_n = -\epsilon_q$, the driven magnons can extract energy from the DW, cooling it toward the ground state, as depicted in Fig. 3(a). The figure shows a pronounced enhancement of the ground-state population compared to the thermal case in Fig. 2(b), demonstrating efficient cooling. Figure 3(c) further shows the out-of-equilibrium ground-state population as a function of DW position for several temperatures, indicating that cooling is most effective when the DW is closer to the left ferromagnetic lead. In contrast, when $\Delta_n = \epsilon_q$, corresponding to magnon frequency down-conversion, the interplay between driven magnons and the anharmonicity of the DW spectrum enhances the population p_2 relative to other DW levels, as shown in Fig. 3(b) for $n = 0$ (lowest magnonic mode). Importantly, such a state can exhibit a negative Wigner function at the origin $W(\Phi = 0, P_\Phi = 0) = \sum_j(-1)^{j+1}p_j$ [30,31], which characterizes a nonclassical DW state (see also [20]). This behavior is illustrated in Fig. 3(d), where the Wigner function is plotted as a function of DW position and is seen to become negative over a broad range of positions and temperatures.

The steady state of a DW can be probed with an additional microwave field, weakly driving one magnonic mode ω_p on resonance, i.e., with $\Omega_p = \omega_p$ (e.g., the $p = 1$ magnonic mode). The power spectrum of the emitted magnons reads

$$\mathcal{S}_p(\omega) = \frac{1}{2\pi}\int_{-\infty}^{\infty} d\tau e^{-i(\omega-\Omega_p)\tau}\langle a_{p,\rm out}^\dagger(t+\tau)a_{p,\rm out}(t)\rangle,$$

where the output field $a_{p,\mathrm{out}}(t)$ is related to the magnonic mode a_p via the standard input-output relation $a_{p,\mathrm{out}}(t) = \sqrt{\kappa_{p,e}}a_p(t) + a_{p,\mathrm{in}}(t)$, and $\langle\cdots\rangle$ denotes the average over the stationary state of the DW. The dynamics of the intracavity field can be described by a quantum Langevin equation [32,33]:

$$\dot{a}_p(t) = -\frac{\kappa_p}{2}a_p(t) + i\frac{P_p(Z_0)P_\Phi}{M_\Phi}a_p(t) - \sqrt{\kappa_{p,e}}a_{p,\mathrm{in}}(t), \quad (12)$$

where $a_{p,\mathrm{in}}(t)$ represents the input field in the probe mode, $\kappa_{p,e}$ the decay rate of mode p into the leads, and all operators are in the Heisenberg picture. Equation (12) can be formally integrated and then subjected to a Dyson series-type expansion to first order in g_p. Assuming $\Gamma^p_{\mathrm{jk}} \ll \Gamma^{\mathrm{tot}}_{\mathrm{jk}}$, such that the measurement does not affect the DW level occupations induced by the other drivings, we find for the sideband transitions (i.e., $\omega \neq \omega_p$) [20]

$$\mathcal{S}_p(\omega) \approx \frac{\kappa_{p,e}}{\pi\kappa_p}\sum_{j,k}\frac{\Gamma^p_{\mathrm{jk}}\Gamma^{\mathrm{eff}}_{\mathrm{jk}}}{(\omega-\Omega_p-\epsilon_{\mathrm{jk}})^2 + \left(\Gamma^{\mathrm{eff}}_{\mathrm{jk}}\right)^2}p_j, \quad (13)$$

where $\Gamma^p_{\mathrm{jk}} = \Gamma^p_{\mathrm{kj}}$ at $\Delta_p = 0$, while $\Gamma^{\mathrm{eff}}_{\mathrm{jk}} = \sum_s(\Gamma^{\mathrm{tot}}_{\mathrm{sk}} + \Gamma^{\mathrm{tot}}_{\mathrm{sj}}) = \Gamma^{\mathrm{eff}}_{\mathrm{kj}}$ represents the peak's linewidth. Consequently, the power spectrum of the emitted magnons exhibits a sideband structure due to the DW-assisted frequency up- or down-conversion processes. For example, when $\Delta_n = -\epsilon_q$ (ground-state cooling), $\mathcal{S}_p(\Omega_p - \epsilon_q)/\mathcal{S}_p(\Omega_p + \epsilon_q) \approx p_1/p_2$, which allows us to infer the ground-state population from the power spectrum of the emitted magnons (together with $\sum_j p_j = 1$).

V. TWO-QUBIT GATES

Magnons can mediate interactions between two such DWs, facilitating the implementation of two-qubit gates. Indeed, assuming that both DWs are cooled down to their respective ground states and that there is sufficient nonlinearity in the spectrum, their dynamics are restricted to the subspace spanned by the lowest two states, $\{|1_a\rangle, |2_a\rangle\}$, with $a = 1, 2$ labeling the DW. In the limit $g_{n,a} \ll ||\Delta_n| - \epsilon_{q,a}| \ll ||\Delta_n| + \epsilon_{q,a}|$ (dispersive regime), we can eliminate perturbatively the magnons (neglecting their decay κ_n) to obtain $H_{1-2} = J_{1-2}(\sigma_1^+\sigma_2^- + \mathrm{H.c.})$, with the exchange coupling

$$J_{1-2} = \frac{2g_{n,1}g_{n,2}|\langle 1_1|P_{1,\Phi}|2_1\rangle||\langle 1_2|P_{2,\Phi}|2_2\rangle|}{\Delta_n - \epsilon_q}, \quad (14)$$

where we assumed identical DWs, and $\sigma_a^+ = |2_a\rangle\langle 1_a|$ ($\sigma_a^- = |1_a\rangle\langle 2_a|$) are the raising (lowering) Pauli operators associated with qubit $a = 1, 2$. Above, we also performed the rotating wave approximation (therefore neglecting terms $\propto \sigma_1^+\sigma_2^+, \sigma_1^-\sigma_2^-$) and disregarded small corrections to each individual qubit Hamiltonian [34]. The evolution of the combined system with H_{1-2} for a time $t_g = \pi/4J_{1-2}$ implements a $\sqrt{i\mathrm{SWAP}}$ operation which, up to single-qubit rotations, is equivalent to a controlled-NOT gate [35]. We consider representative parameters $\varepsilon_q \simeq 0.1$ GHz (quartic point) and Gilbert damping $\alpha = 10^{-5}$ (YIG-like), corresponding to an intrinsic magnon linewidth $\kappa_n \lesssim$ MHz at GHz frequencies, i.e., in the resolved-sideband regime. At $T = 0.05$ K, the thermal DW relaxation rate is $\gamma_{12} \approx 10^{-3}\varepsilon_q$. We then choose a dispersive offset $\delta = |\Delta_n - \varepsilon_q| = 0.2\,\varepsilon_q$ and $|\alpha_n| = 0.6$, corresponding to an intracavity magnon number ∼0.36. Assuming $P_n(-Z_0) \sim 1$ for both domain walls, Equation (14) yields $J_{1-2} \sim 7$ MHz. This corresponds to a $\sqrt{i\mathrm{SWAP}}$ gate duration of $t_g \approx 100$ ns, which is comfortably shorter than the domain-wall relaxation time $T_1 \sim 1/\gamma_{12} \approx 1.6$ μs at this temperature. Given that $\kappa_n \ll \delta$, the cavity-induced dephasing during the gate operation is negligible, while heating remains minimized due to the dispersive detuning. In combination with single-qubit gates, which are achievable through the local application of ac magnetic field pulses, the interaction H_{1-2} is therefore sufficient for universal quantum computation.

VI. CONCLUSIONS AND OUTLOOK

In summary, we have shown that magnons in short insulating ferromagnetic wires can be leveraged to initialize, entangle, and detect quantum states encoded in macroscopic DWs. These features are enabled by universal (and intrinsic) Coriolis-type interactions between the magnons and the DW, rendering our approach promising in terms of scalability since it does not require extrinsic degrees of freedom (e.g., photons) to be integrated with the ferromagnetic wire. By the same token, it could be naturally extended to two-dimensional topological objects, such as skyrmions [10], or even to other magnetic materials, such as ferrimagnets or antiferromagnets, which can exhibit faster timescales for manipulation. Looking ahead, it would be interesting to extend our approach to the effective quantization of collective coordinates to account for the intrinsic quantumness of domain walls and magnons, such as those emerging in spin-1/2 quantum magnets [36–38].

ACKNOWLEDGMENTS

The authors acknowledge fruitful discussions with Dalton Jones in the early stages of this work. This work was supported by the Foundation for Polish Science project MagTop (Grant No. FENG.02.01IP.05-0028/23) cofinanced by the European Union from the funds of Priority 2 of the European Funds for a Smart Economy Program 2021-2027 (FENG) (M.T.), by the National Science Centre (Poland) OPUS Grant No. 2021/41/B/ST3/04475 (M.T.), by the NAWA Bekker Grant No. BPN/BEK/2024/1/00310 (Poland) (M.T.), and NSF under Grant No. DMR-2049979 (Y.T.).

DATA AVAILABILITY

The data that support the findings of this article are not publicly available. The data are available from the authors upon reasonable request.

[1] J. Zang, V. Cros, and A. Hoffmann, *Topology in Magnetism*, Springer Series in Solid-State Sciences (Springer International Publishing, Cham, Switzerland, 2018), Vol. 192 .

[2] G. S. D. Beach, C. Nistor, C. Knutson, M. Tsoi, and J. L. Erskine, Dynamics of field-driven domain-wall propagation in ferromagnetic nanowires, Nat. Mater. **4**, 741 (2005).

[3] M. Hayashi, L. Thomas, R. Moriya, C. T. Rettner, and S. S. P. Parkin, Current-controlled magnetic domain-wall nanowire shift register, Science **320**, 209 (2008).

[4] S. S. P. Parkin, M. Hayashi, and L. Thomas, Magnetic domain-wall racetrack memory, Science **320**, 190 (2008).

[5] J. Grollier, D. Querlioz, K. Y. Camsari, K. Everschor-Sitte, S. Fukami, and M. D. Stiles, Neuromorphic spintronics, Nat. Electron. **3**, 360 (2020).

[6] D. Kumar, T. Jin, R. Sbiaa, M. Kläui, S. Bedanta, S. Fukami, D. Ravelosona, S.-H. Yang, X. Liu, and S. Piramanayagam, Domain wall memory: Physics, materials, and devices, Phys. Rep. **958**, 1 (2022).

[7] S. Takei, Y. Tserkovnyak, and M. Mohseni, Spin superfluid Josephson quantum devices, Phys. Rev. B **95**, 144402 (2017).

[8] S. Takei and M. Mohseni, Quantum control of topological defects in magnetic systems, Phys. Rev. B **97**, 064401 (2018).

[9] I. Proskurin, A. S. Ovchinnikov, J.-i. Kishine, and R. L. Stamps, Cavity optomechanics of topological spin textures in magnetic insulators, Phys. Rev. B **98**, 220411 (2018).

[10] C. Psaroudaki and C. Panagopoulos, Skyrmion qubits: A new class of quantum logic elements based on nanoscale magnetization, Phys. Rev. Lett. **127**, 067201 (2021).

[11] P. Siegl, E. Y. Vedmedenko, M. Stier, M. Thorwart, and T. Posske, Controlled creation of quantum skyrmions, Phys. Rev. Res. **4**, 023111 (2022).

[12] J. Zou, S. Bosco, B. Pal, S. S. P. Parkin, J. Klinovaja, and D. Loss, Quantum computing on magnetic racetracks with flying domain wall qubits, Phys. Rev. Res. **5**, 033166 (2023).

[13] G. Tatara, H. Kohno, and J. Shibata, Microscopic approach to current-driven domain wall dynamics, Phys. Rep. **468**, 213 (2008).

[14] M. Aspelmeyer, T. J. Kippenberg, and F. Marquardt, Cavity optomechanics, Rev. Mod. Phys. **86**, 1391 (2014).

[15] S. Sharma, Y. M. Blanter, and G. E. W. Bauer, Optical cooling of magnons, Phys. Rev. Lett. **121**, 087205 (2018).

[16] J. Graf, H. Pfeifer, F. Marquardt, and S. V. Kusminskiy, Cavity optomagnonics with magnetic textures: Coupling a magnetic vortex to light, Phys. Rev. B **98**, 241406 (2018).

[17] M. J. Martínez-Pérez and D. Zueco, Strong coupling of a single photon to a magnetic vortex, ACS Photon. **6**, 360 (2019).

[18] M. J. Martínez-Pérez and D. Zueco, Quantum electrodynamics with magnetic textures, New J. Phys. **21**, 115002 (2019).

[19] J. O. Iyaro, I. Proskurin, and R. L. Stamps, Collective dynamics of domain walls: An antiferromagnetic spin texture in an optical cavity, Phys. Rev. B **104**, 184416 (2021).

[20] See Supplemental Material at http://link.aps.org/supplemental/10.1103/h876-wl85 for details on the derivation of the DW Hamiltonian, the interaction with the magnons, and the evolution of the combined system under microwave drivings, which includes Refs. [39,40].

[21] H. P. Breuer and F. Petruccione, *The Theory of Open Quantum Systems* (Oxford University Press, Oxford, 2002).

[22] S. K. Kim, O. Tchernyshyov, V. Galitski, and Y. Tserkovnyak, Magnon-induced non-Markovian friction of a domain wall in a ferromagnet, Phys. Rev. B **97**, 174433 (2018).

[23] This result is strictly valid only for magnons with wave vectors satisfying $kL \gg 1$; for magnons with $kL \sim 1$, this simple picture remains qualitatively correct, but it is affected slightly by interference effects, as demonstrated in Ref. [20].

[24] The presence of a magnetic field and easy-axis anisotropy causes extra DW-magnon interactions of Hamiltonian origin, but they scale as $\propto 1/L$ [20], and hence are subleading as compared to the Coriolis-type contribution.

[25] A. A. Kovalev and Y. Tserkovnyak, Thermomagnonic spin transfer and Peltier effects in insulating magnets, Europhys. Lett. **97**, 67002 (2012).

[26] K. A. van Hoogdalem, Y. Tserkovnyak, and D. Loss, Magnetic texture-induced thermal Hall effects, Phys. Rev. B **87**, 024402 (2013).

[27] N. Nagaosa, Emergent electromagnetism in condensed matter, Proc. Jpn. Acad. Ser. B **95**, 278 (2019).

[28] The long-wavelength magnons are practically unaffected by the pinning potential because their amplitude is negligible at the position of the scatterer $Z = Z_0$ (see also Ref. [20]).

[29] I. Wilson-Rae, N. Nooshi, J. Dobrindt, T. J. Kippenberg, and W. Zwerger, Cavity-assisted backaction cooling of mechanical resonators, New J. Phys. **10**, 095007 (2008).

[30] S. Rips, M. Kiffner, I. Wilson-Rae, and M. J. Hartmann, Steady-state negative Wigner functions of nonlinear nanomechanical oscillators, New J. Phys. **14**, 023042 (2012).

[31] S. Haroche and J. M. Raimond, *Exploring the Quantum: Atoms, Cavities, and Photons* (Oxford University Press, Oxford, 2006).

[32] A. A. Clerk, M. H. Devoret, S. M. Girvin, F. Marquardt, and R. J. Schoelkopf, Introduction to quantum noise, measurement, and amplification, Rev. Mod. Phys. **82**, 1155 (2010).

[33] S. Rips, I. Wilson-Rae, and M. J. Hartmann, Nonlinear nanomechanical resonators for quantum optoelectromechanics, Phys. Rev. A **89**, 013854 (2014).

[34] S. Rips and M. J. Hartmann, Quantum information processing with nanomechanical qubits, Phys. Rev. Lett. **110**, 120503 (2013).

[35] A. Barenco, C. H. Bennett, R. Cleve, D. P. DiVincenzo, N. Margolus, P. Shor, T. Sleator, J. A. Smolin, and H. Weinfurter, Elementary gates for quantum computation, Phys. Rev. A **52**, 3457 (1995).

[36] R. Schilling, Quantum theory of domain walls, Phys. Rev. B **15**, 2700 (1977).

[37] H. Y. Yuan, M.-H. Yung, and X. R. Wang, Emergence of antiferromagnetic quantum domain walls, Phys. Rev. B **98**, 060407 (2018).

[38] G. Qu, J. Zou, D. Loss, and T. Hirosawa, Density matrix renormalization group study of domain wall qubits, Phys. Rev. B **112**, 054432 (2025).

[39] A. Altland and B. D. Simons, *Condensed Matter Field Theory* (Cambridge University Press, Cambridge, United Kingdom, 2010).

[40] C. W. Gardiner and P. Zoller, *Quantum Noise*, 2nd ed. (Springer, Berlin, Germany, 2000)